Activity and Stability of Novel Silica-Based Catalysts for Hydrogen Production via Oxidative Steam Reforming of Ethanol

Vincenzo Palma, Concetta Ruocco*, Eugenio Meloni, Antonio Ricca

University of Salerno, D. I. In., Via Giovanni Paolo II 132, 84084 Fisciano (SA), Italy
cruocco@unisa.it

The development of catalysts resistant to deactivation, especially to coke formation, is a key issue to perform ethanol reforming successfully. Aiming at carbon formation minimization, in the present work, bimetallic Pt-Ni/CeO$_2$ catalysts were deposited on silica gel with high surface area and tested for ethanol reforming in the low temperature range (300 - 600 °C). The activity was investigated at different contact times and the impact of oxygen co-feeding on catalyst performances was also studied. The increase of space velocity had no effect on ethanol conversion at T > 420 °C under both oxidative and non-oxidative conditions; however, when O$_2$ was co-fed, contact time growth assured almost total conversion until 300 °C. Moreover, the results of stability tests revealed that O$_2$ addition in the reforming mixture improved catalyst stability, which was maintained for 70 h.

1. Introduction

In view of the increasing exploitation of energetic sources by both domestic and industrial users, finding clean technologies for energy production have received a huge attention (Silva et al., 2015). Moreover, in order to lower pollutants and greenhouse generation, a drastic reduction of fossil fuels dependence is mandatory. Hydrogen produced from renewable feed-stocks is a carbon-free fuel able to provide clean electricity in fuel cells devices, with water being the only by-product (Beheshti et al., 2016). In this perspective, H$_2$ production via biofuels conversion attracted much attention, as the CO$_2$ formed during the reaction can be reused in plant growth cycle. Among the different biomass derived liquids, ethanol was widely reported as hydrogen source to be converted through different technologies including steam reforming (ESR), partial oxidation and oxidative steam reforming (OSR). Partial oxidation assures low temperature operations but, as a drawback, the high exothermicity may cause hot spots formation and catalyst deactivation (de Ávila et al. 2011). On the other hand, ESR, despite providing high H$_2$ yields, due to the reaction endothermicity, is characterized by relevant capital and operational costs. Conversely, OSR (i.e. a combination of steam reforming and partial oxidation) displays two significant benefits: the exothermic contribution of oxidation reactions may reduce the external heat supply and air co-feeding tends to decrease carbon deposits on catalysts (Sun et al., 2012).
The general equation for ethanol reforming reaction can be written as reported in Eq(1), where a = 0 for ESR.

$$C_2H_5OH + (3 - 2a)H_2O + aO_2 \leftrightarrow (6 - 2a)H_2 + 2CO_2 \tag{1}$$
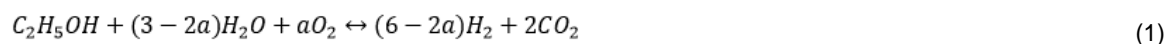
Under oxidative reaction, besides providing required heat amounts depending on the a value, it is also possible to reduce the formation of carbon monoxide, a well-known poison for the catalyst of certain fuel cells. However, for both ESR and OSR, various reaction pathways may operate, on the basis of the selected catalyst as well as operative conditions. Different authors tested noble metals (Mironova et al., 2014) and transition metals (Gu et al., 2013) supported on numerous oxides for reforming of ethanol. Ceria has been widely employed as catalytic support due to its oxygen storage properties, which improves catalyst stability. Moreover, CeO$_2$ promotes metal-support interactions, thus preventing sintering phenomena. The employment of non-precious metals, although showed inferior catalytic performances than noble metals, is encouraged by

their low cost. However, the addition of small precious metals amounts to Ni-based catalyst was shown to improve water gas shift activity as well as deactivation resistance (Mondal et al., 2015). The superior catalytic performances of bimetallic formulations compared to monometallic is well documented (Contreras et al., 2014).

In the present work, a Pt-Ni/CeO_2 system was deposited on silica gel having high surface area in order to improve active species dispersion, which is expected to enhance catalytic performances. The samples were tested for oxidative and non-oxidative reforming of ethanol at different space velocities and the impact of oxygen co-feeding on ethanol conversion as well as catalyst stability was investigated.

2. Experimental

2.1 Preparation and characterization of the catalyst

The silica gel support, provided by Sigma-Aldrich, before CeO_2 deposition, was calcined at 600 °C for 3 h (heating rate of 10 °C min^{-1}) in a muffle furnace in order to remove impurities from catalyst surface. Then, the cerium nitrate ($Ce(NO_3)_3*6H_2O$), nickel nitrate ($Ni(NO_3)_2*6H_2O$) and platinum chloride ($PtCl_4$), supplied by Strem Chemicals, were sequentially impregnated through the wetness method. The solid was stirred in the aqueous solution of the corresponding salt, heated at 80 °C for 2 h on plate and finally separated by means of a Buchner funnel. After each impregnation, the sample was dried overnight and calcined at the same conditions reported for SiO_2. Different impregnations were performed to reach CeO_2, Ni and Pt loadings which were fixed to 20 wt%, 10 wt% and 3 wt%, respectively. Metals contents are referred to the total ceria mass. Impregnation order (Ni earlier than Pt) and metals loadings were previously optimized for SiO_2-free catalysts (Palma et al., 2011).

The CeO_2, Ni and Pt loadings were measured by X-ray fluorescence (XRF) spectrometry in a ThermoFischer QUANT'X EDXRF spectrometer equipped with a rhodium standard tube as the source of radiation. BET surface areas were measured by N_2 physisorption at its normal boiling point in a Sorptometer 1040 "Kelvin" from Costech Analytical Technologies. XRD patterns were registered on D-8 Advance Bruker WAXRD diffractometer (λ = 1.5406 A˚). The diffractograms were recorded between 5 and 80°. A Dispersive MicroRaman (Invia, Renishaw), equipped with 785 nm diode-laser, was employed for the production of Raman Spectra. TPR (Temperature Programmed Reduction) measurements were carried out in the laboratory apparatus describe in Par. 2.2. Temperature was increased to 600 °C (heating rate of 10 °C min^{-1}) under a 5 %H_2 in N_2 stream; after the ramp, the sample was held at the maximum temperature for 1 h in the reducing atmosphere. The spent catalysts after stability tests were characterized by thermo-gravimetric analysis (TGA), in order to evaluate the deposited carbon. The instrument employed was a Q600, TA Instrument, coupled with a PFEIFFER Mass Spectrometer.

2.2 Reforming tests

Catalytic tests were conducted in a tubular annular stainless steel reactor (e.d. = 19 mm, i.d. = 17 mm) at atmospheric pressure and moderate temperatures (300-600 °C); the catalyst, crushed and sieved in order to reach a 180 - 355 µm granulometry, was held between two quartz flakes and placed in the reactor annular section. The reactor was vertically positioned inside an electrical furnace and the temperature was monitored through a thermocouple placed at the center of catalyst end section. After hydrogen reduction in situ, the water/ethanol mixture (molar ratio = 4), properly diluted with N_2, was sent to a boiler for vaporization and then to the reactor. During oxidative tests, air was directly fed to reactor through an independent line. All the tests were performed at a total flow-rate of 550 Ncm^3 min^{-1} (10 % C_2H_5OH – 40 % N_2 – 50 % N_2 for ESR and 10 % C_2H_5OH – 5 % O_2 – 45 % N_2) and the proper space velocity was settled by changing catalytic volume. All the lines downstream the boiler are heated at 140 °C and a system of 5 heated solenoids allowed the switch between reaction and by-pass configuration. In the latter case, it is also possible to wash the reactor through an independent N_2 line. The gaseous products (C_2H_5OH, H_2O, CO, CO_2 and CH_4) were analyzed on-line through an FT-IR Spectrophotometer (Nicolet Antaris IGS by ThermoScientific). The effluents from Nicolet were cooled by passing through a condensation system, in order to assure the normal operation of downstream analysis equipment. hydrogen and oxygen dry concentrations in the reforming mixture were determined by a thermoconductivity ABB-CALDOS 27 and a continuous paramagnetic analyser ABB-MAGNOS 206, respectively.

The results of activity tests, carried out between 300 and 600°C and at space velocity (GHSV) values ranging from 100,000 and 300,000 h^{-1}, were compared in terms of ethanol conversion, X (Eq(2)) and hydrogen yield, Y (Eq(3)).

$$X = \frac{mol_{C2H5OH,in} - mol_{C2H5OH,out}}{mol_{C2H5OH,in}} \qquad (2) \qquad Y = \frac{mol_{H2}}{6 * mol_{C2H5OH,in}} \qquad (3)$$

$$CFR = \frac{m_{coke}}{m_{carbon,fed} \, m_{cat} * TOS}$$

(4)

On the basis of characterization results (Par. 3.1), which suggests that ceria forms a substrate over-layer on SiO_2, the equivalent catalytic volume of $Ni+Pt+CeO_2$ was taken into account for the calculation of GHSV. Moreover, for the catalyst durability tests, performed at 500 °C and 20,000 h^{-1}, the coke formation resistance during ESR and OSR was evaluated through the carbon formation rate (CFR, Eq.4) parameter, defined as the coke mass detected trough thermo-gravimetric analysis normalized with respect to the total mass of carbon fed during the test, the catalytic mass and the time on stream (TOS).

3. Results and discussion

3.1 Characterization of the Pt-Ni/CeO₂/SiO2 catalyst

Physiochemical properties of the CeO_2/SiO_2 support as well as the final catalyst are reported in Table 1. XRF analysis revealed a fairly good agreement between experimental and theoretical loadings (2.22 and 0.60 corresponds, respectively, to 9.7 and 2.6 wt% with respect to CeO_2). Ceria impregnation reduced SiO_2 SSA (400 m^2/g after calcination at 600 °C) of almost 30 %. However, active species deposition caused a less pronounced variation (from 281 to 232 m^2/g). In Figure 1(a), the XRD pattern of the fresh catalyst is presented along with the spectrum of the CeO_2/SiO_2 sample. An amorphous peak at around 23°, assigned to SiO_2, was observed in both the patterns. The CeO_2/SiO_2 sample and the ceria-containing catalyst also showed reflections corresponding to the face-centered cubic structure of CeO_2 (Zhang et al., 2015) while the peaks observed at 37.3, 43.3, 63.1° can be assigned to NiO. No reflections attributed to PtO_x were visible, suggesting that Pt particles are too small to be detected. The size of ceria particles (7 nm) was not affected during preparation procedure and the crystallite dimension of NiO particles was about 11 nm.

Table 1: XRF, BET and XRD results.

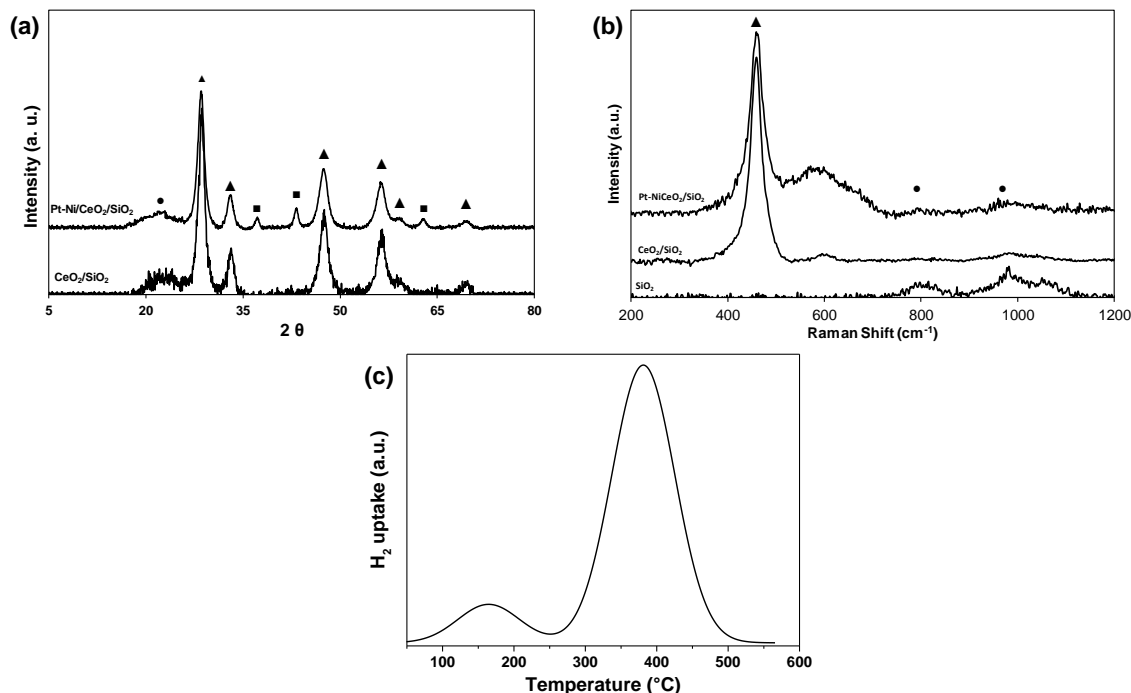| Sample	SSA (m^2/g)	CeO₂ wt%	Ni wt%	Pt wt%	d$_{CeO2}$ (Å)	d$_{NiO}$ (Å)
CeO₂/SiO₂	281	21.3	-	-	67	-
Pt-Ni/CeO₂/SiO₂	232	20.7	2.22	0.60	68	114

Figure 1: (a) XRD and (b) Raman spectra of the support and the catalyst (●SiO₂, ▲CeO₂, ■NiO); (c) deconvoluted TPR profile over Pt-Ni/CeO₂-SiO₂ catalyst

The results of XRD analysis of both the support and the final catalyst displayed no shift in SiO_2 and CeO_2 peaks showing that no mixed oxide formation occurred. The same observation can be drawn from the Raman

spectra (Figure 1(b)) suggesting that silica forms a substrate while ceria has been forming a surface over-layer (Reddy et al., 2002). Moreover, after ceria deposition, a strong attenuation of SiO_2 peaks (Figure 1(b)) was observed, further strengthening the above hypothesis.

The H_2-TPR profile of the bimetallic catalyst (Figure 1 (c)) displays two reduction peaks at 164 and 381°C, representing, respectively, PtO_x and NiO reduction. Hydrogen consumptions, estimated from the area under the two peaks by means of the Software Origin, were equal to 513 and 3,770 $\mu molH_2/g_{cat}$, respectively for Pt and Ni.

Both the values exceeded the theoretical uptakes (308 and 1,704 $\mu mol/g_{cat}$): the dissociation of hydrogen molecules over the Pt sites and the spillover of H_2 to nickel and cerium oxide is responsible for an earlier reduction of NiO at low temperatures; moreover, such just reduced Pt and/or Ni particles also catalyze a beforehand surface reduction of CeO_2. It's also worthwhile noting that the high oxygen storage and release capacity of the support may further enhance the catalyst reducibility (Moraes et al. 2016).

3.2 Comparison of catalyst performances for steam and oxidative steam reforming of ethanol

The performances of Pt-Ni bimetallic catalysts for ESR and OSR were preliminary compared in terms of ethanol conversion and hydrogen yields between 300 and 600 °C and at different space velocities (GHSV = 10,000 - 30,000 h^{-1}). The results are summarized in Table 2.

Table 2: Detailed catalytic activity of Pt-Ni/CeO_2/SiO_2 during steam and oxidative steam reforming of ethanol (Y_{eq} stands for equilibrium yield); r.a.=4, r.o.=0.5

		ESR			OSR		
GHSV (h^{-1})	T (°C)	X (%)	Y (%)	Y_{eq} (%)	X (%)	Y (%)	Y_{eq} (%)
10,000	600	100	71.6	70.4	100	65.5	63.9
	500	100	42.5	43.4	100	42.5	41.5
	400	100	28.7	19.1	100	26.3	18.2
	300	82.7	18.2	5.46	100	13.4	5.07
20,000	600	100	70.7	70.4	100	64.1	63.9
	500	100	42.9	43.4	100	42.5	41.5
	400	100	27.1	19.1	100	27.2	18.2
	300	61.6	12.0	5.5	65.1	6.05	5.1
30,000	600	100	70.2	70.4	100	65.1	63.9
	500	100	42.2	43.4	100	42.8	41.5
	400	100	24.8	19.1	100	25.3	18.2
	300	27.4	7.5	5.5	40.8	2.4	5.1

Total ethanol conversion was recorded in the temperature interval of 400 - 600 °C and space velocity as well as oxygen co-feeding had no effect on this results. Moreover, hydrogen yields fairly agreed with thermodynamic predictions (70.4 % and 63.9 % for ESR and OSR at 600 °C, respectively) during both oxidative and non-oxidative tests at T > 500 °C. However, as previously discussed (Palma et al., 2015), in the low-temperature range, H_2 yields are quite far from equilibrium predictions: the higher contribution of water gas shift reaction with respect to methanation led to an increase in hydrogen production rate.

Concerning steam reforming tests, the reduction of contact time negatively affected ethanol conversion at 300 °C, which dropped from 82.7 % at 10,000 h^{-1} to 27.4 % at 30,000 h^{-1}. Conversely, during oxidative reforming over Pt-Ni/CeO_2/SiO_2 catalysts, at the highest contact time, X was equal to 100 % even at 300 °C while a less pronounced reduction in ethanol conversion (from 65.1 % to 40.8 %) was observed at 20,000 and 30,000 h^{-1}. Moreover, a deceasing trend in H_2 yields at 300 °C along with the growth in space velocity was observed: the reduction in ethanol moles converted was responsible for a lower hydrogen production. It's also interesting to note that oxygen (not shown) was completely converted, independently from temperature and space velocity.

The relevant ethanol conversions recorded under both ESR and OSR tests are linked to the promotion of C-C bonds breaking by Nickel as well as ceria (Kugai et al., 2006). Moreover, oxygen co-feeding enhanced the rate of oxidation reactions promoting the conversion of C-containing species to CO_2 (Morales et al., 2015).

In order to investigate the effect of oxygen co-feeding on catalytic performances, stability tests were performed at an intermediate GHSV (20,000 h^{-1}) and 500°C. Product gas distribution well agreed with thermodynamic data (the equilibrium concentration of C_2H_5OH was omitted, as a total conversion is predicted at the investigated conditions) and no sensible variations were observed for almost 2,000 min during ESR (Figure 3(a)) and 3,000 min for the OSR test (Figure 3(b)). The selected catalyst displayed high durability in both the cases and total ethanol conversion was recorded for more than 40 h under steam reforming conditions. However, oxygen co-feeding strongly improved catalyst stability, resulting in 100 % of C_2H_5OH conversion for

almost 60 h. Despite the above difference, the mechanism which led to catalyst deactivation was similar for the two systems: a slight increase in CO concentration was observed and a concomitant decrease of CO_2 levels as well as a growth of water concentration well agreed with the stoichiometry of reverse water gas shift reaction. A reduction was also recorded for CH_4 concentration, which, according to a decrease in H_2 concentration slower than that dictated by reverse WGS stoichiometry, was due to methane decomposition reactions. As a consequence, coke formation increased, leading to catalyst deactivation.
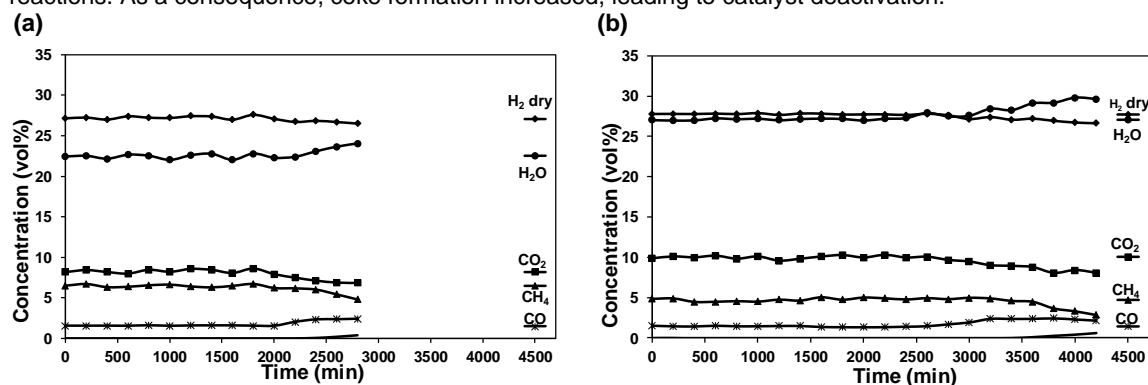
(a)   **(b)**

Figure 3: Product gas distribution as a function of time-on-stream for steam (a) and oxidative (b) reforming reaction; r.a.= 4, r.o.= 0.5, T = 500 °C, GHSV = 20,000 h^{-1}

However, it's worthwhile noting that the O_2 availability enhanced the removal of deposited carbon, detrimental for catalyst stability, resulting, at the same time, in H_2 productivities very close to the values recorded in the absence of oxygen. In fact, the average yields were equal to 41.7 % and 43.6 % for ESR and OSR.

In order to demonstrate that the difference in catalyst stability is only ascribable to carbonaceous deposits, the exhaust samples were characterized by means of XRD analysis. No variation on the average crystallite sizes of ceria was observed, thus averting sintering phenomena occurring. Moreover, in the spectra of the spent catalysts (Figure 4(a)), only the peak of metallic nickel at 44.5 ° (Zhou et al., 2015) is visible along with ceria fluorite structure. Conversely, the NiO species were only detected over the fresh sample, proving that the reduction procedure assured the proper conversion of nickel oxide to the metallic form. Due to the relative low operating temperatures, no peaks ascribable to the formation of graphitic carbon (Rajarao et al., 2016) were observed, demonstrating that the coke detected through thermos-gravimetric analysis was not in a crystalline form.
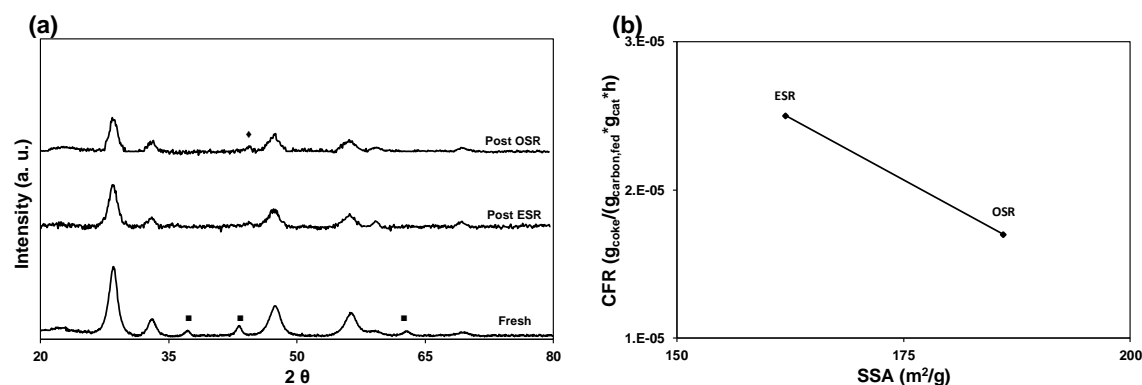
(a)   **(b)**

Figure 4: (a) Comparison between the diffraction patterns of fresh and spent catalysts (■NiO, ♦ Ni); (b) relationship between carbon formation rate and specific surface area of the spent samples

During time-on-stream tests, a pronounced reduction in specific surface area with respect to the fresh catalysts, which displayed a SSA of 232 m^2/g, was observed for both steam and oxidative steam reforming conditions (Figure 4(a)). However, this effect was less evident over the catalyst tested under oxidative reforming conditions, which also displayed a reduction in carbon formation rate of almost 30 % (1.7 vs 2.5*10^5 g_{coke}/($g_{carbon,fed}$*g_{cat}*h). Oxygen co-feeding, in fact, enhanced coke gasification reaction as well as catalyst surface cleaning. However, as previously reported (Hou et al., 2015), it's worthwhile highlighting that the employment of earth species as catalytic supports, due to their oxygen storage-release capability, assured very high resistance to coke formation in both the cases.

4. Conclusions

In this study, the catalytic activity of Pt-Ni/CeO_2/SiO_2 catalysts towards ethanol reforming was investigated. Complete conversion of ethanol along with a fair hydrogen yield was recorded between 400 and 600 °C during both oxidative and non-oxidative tests. However, at lower temperature, the reduction of contact time was detrimental for catalyst activity, resulting in reduced conversion especially during steam reforming tests. On the other hand, at 10,000 h^{-1}, r.a. = 4 and r.o. = 0.5, C_2H_5OH was completely converted in the interval 300 - 600 °C The samples, tested at 500 °C and 20,000 h^{-1}, displayed a good resistance to deactivation and a stable behavior for at least 40 h. Both the catalysts suffered of a surface area reduction during stability tests, more pronounced for the ESR case, which, however, was not caused by sintering phenomena. On the other hand, oxygen co-feeding strongly improved catalyst durability, resulting in a carbon formation rate reduction of almost 30 %.

Acknowledgments

References

Beheshti S.M., Ghassemi H., Shahsavan-Markadeh R., 2016, An advanced biomass gasification-proton exchange membrane fuel cell system for power generation, J. Clean. Prod., 112, 995-100.

Contreras J.L., Salmones J., Nuno L., Cordova I., Zeifert B., Tapia C., Fuentes G.A., 2014, Catalysts for H_2 production using the ethanol steam reforming. Int. J. Hydrogen Energy, 39, 18835-18853.

de Ávila C.N., Hori C.E., de Assis A.J., 2011, Thermodynamic assessment of hydrogen production and cobalt oxidation susceptibility under ethanol reforming conditions, J. Clean. Prod., 36, 4385-4395.

Gu R., Zeng G., Shao J., Liu Y., Schwank J.W., Li Y., 2013, Sustainable H_2 production from ethanol steam reforming over a macro-mesoporous Ni/Mg-Al-O catalytic monolith, Front. Chem. Sci. Eng., 7, 270–278.

Hou T., Zhang S., Chen Y., Wang D., Cai W., 2015, Hydrogen production from ethanol reforming: Catalysts and reaction mechanism, Renew. Sust. Energ. Rev., 44, 132–148.

Kugai J., Subramani V., Chin Y.-H., 2006, Effects of nanocrystalline CeO_2 supports on the properties and performance of Ni–Rh bimetallic catalyst for oxidative steam reforming of ethanol, J. Catal., 238, 430–440.

Mironova E.Y., Ermilova M.M., Orekhova N.V., Muraviev D.N., Yaroslavtseva A.B., 2014, Production of high purity hydrogen by ethanol steam reforming in membrane reactor, Catal. Today, 236, 64-69.

Mondal T., Pant K.K., Dalai A.K., 2015, Catalytic oxidative steam reforming of bio-ethanol for hydrogen production over Rh promoted Ni/CeO_2-ZrO_2 catalyst, Int. J. Hydrogen Energy, 2529-2544.

Moraes T.S., Ribeiro M., Mattos L., Verykios X., Noronha F., 2016, Ethanol conversion at low temperature over CeO_2-Supported Ni-based catalysts. Effect of Pt addition to Ni catalyst, Appl. Catal B: Environ., 181, 754-768.

Morales M., Segarra M., 2015, Steam reforming and oxidative steam reforming of ethanol over $La_{0.6}Sr_{0.4}CoO_{3-\delta}$ perovskite as catalyst precursor for hydrogen production, Appl. Catal. A: Gen., 502, 305–311.

Palma V., Palo E., Castaldo F., Ciambelli P., Iaquaniello G., 2011, Catalytic activity of CeO_2 supported Pt-Ni and Pt-Co catalysts in the low temperature bioethanol steam reforming, Chem. Eng. Trans., 17, 947-952.

Palma V., Ruocco C., Ricca A., 2015, Bimetallic Pt and Ni Based Foam Catalysts for Low-Temperature Ethanol Steam Reforming Intensification, Chem. Eng. Trans., 43, 559-564.

Rajarao R., Sahajwalla V., 2016, A cleaner sustainable approach for synthesising high purity silicon carbide and silicon nitride nanopowders using macadamia shell waste, J. Clean. Prod., 133, 1277-1284.

Reddy B.M., Khan A., Yamada Y., Kobayashi T., Volta J.-C., 2002, Surface Characterization of CeO_2/SiO_2 and V_2O_5/CeO_2/SiO_2 Catalysts by Raman, XPS, and Other Techniques, J. Phys. Chem. B, 106, 10964-10972.

Silva F.R., Silva J.D., 2015, Catalytic Steam Reforming Pos-Gasification Using Toluene as Model Compound, Chem. Eng. Trans., 43, 2023-2028.

Sun S., Yan W., Sun P., Chen J., 2012, Thermodynamic analysis of ethanol reforming for hydrogen production, Energy 44, 911-924.

Zhang M., Xiao M., Han D., Lu Y., Meng Y., 2015, Cerium oxide-based catalysts made by template-precipitation for the dimethyl carbonate synthesis from Carbon dioxide and methanol, J. Clean. Prod.,103, 847-853.

Zhou Y., Wang S., Xiao M., Han D., Lu Y., Meng Y., 2015, Formation of Dimethyl Carbonate on Nature Clay Supported Bimetallic Copper-Nickel Catalysts, J. Clean. Prod., 103, 925-933.